The Dynamics of Genetic Interactions Between Vibrio metoecus and Vibrio cholerae, Two Close Relatives Co-Occurring in the Environment

Fabini Orata, Paul Kirchberger, Raphaël Méheust, E. Jed Barlow, Cheryl L. Tarr, Yan Boucher

HAL Id: hal-01264332

https://hal.sorbonne-universite.fr/hal-01264332v1

Submitted on 29 Jan 2016

The Dynamics of Genetic Interactions Between *Vibrio metoecus* and *Vibrio cholerae*, Two Close Relatives Co-Occurring in the Environment

Fabini D. Orata[1], Paul C. Kirchberger[1], Raphaël Méheust[2], E. Jed Barlow[3], Cheryl L. Tarr[4], Yan Boucher[1],*

[1]Department of Biological Sciences, University of Alberta, Edmonton, Alberta, Canada

[2]Unité Mixte de Recherche 7138, Evolution Paris-Seine, Institut de Biologie Paris-Seine, Université Pierre et Marie Curie, Paris, France

[3]Department of Computing Science, University of Alberta, Edmonton, Alberta, Canada

[4]National Center for Emerging and Zoonotic Infectious Diseases, Centers for Disease Control and Prevention, Atlanta, Georgia, USA

*Corresponding author: Yan Boucher, Department of Biological Sciences, University of Alberta, Edmonton, Alberta T6G 2E9, Canada; yboucher@ualberta.ca

Running title: Genetic Interactions Between *V. metoecus* and *V. cholerae*

ABSTRACT

Vibrio metoecus is the closest relative of *Vibrio cholerae*, the causative agent of the potent diarrheal disease cholera. Although the pathogenic potential of this new species is yet to be studied in depth, it has been co-isolated with *V. cholerae* in coastal waters and found in clinical specimens in the USA. We used these two organisms to investigate the genetic interaction between closely related species in their natural environment. The genomes of twenty *V. cholerae* and four *V. metoecus* strains isolated from a brackish coastal pond on the US east coast, as well as four clinical *V. metoecus* strains were sequenced and compared to reference strains. Whole genome comparison shows 86-87% average nucleotide identity (ANI) in their core genes between the two species. On the other hand, the chromosomal integron, which occupies approximately 3% of their genomes, shows higher conservation in ANI between species than any other region of their genomes. The ANI of 93-94% observed in this region is not significantly greater within than between species, meaning that it does not follow species boundaries. *V. metoecus* does not encode toxigenic *V. cholerae* major virulence factors, the cholera toxin and toxin co-regulated pilus. However, some of the pathogenicity islands found in pandemic *V. cholerae* were either present in the common ancestor it shares with *V. metoecus*, or acquired by clinical and environmental *V. metoecus* in partial fragments. The virulence factors of *V. cholerae* are therefore both more ancient and more widespread than previously believed. There is high interspecies recombination in the core genome, which has been detected in 24% of the single-copy core genes, including genes involved in pathogenicity. *V. metoecus* was six times more often the recipient of DNA from *V. cholerae* as it was the donor,

indicating a strong bias in the direction of gene transfer in the environment.

Key words: *Vibrio metoecus*, *Vibrio cholerae*, horizontal gene transfer, genomic islands, integron, comparative genomics

INTRODUCTION

The genus *Vibrio* constitutes a diverse group of gammaproteobacteria ubiquitous in marine, brackish, and fresh waters. There are currently over 100 species of vibrios that have been described (Gomez-Gil et al. 2014). This includes clinically significant pathogens such as *V. cholerae*, *V. parahaemolyticus*, and *V. vulnificus* among many others. *V. cholerae*, the causative agent of the potent diarrheal disease cholera, is the most notorious of these human pathogens. Cholera remains a major public health concern, with an estimated 1.2 to 4.3 million cases and 28,000 to 142,000 deaths every year worldwide (Ali et al. 2012).

A novel *Vibrio* isolate, initially identified as a nonpathogenic environmental variant of *V. cholerae* (Choopun 2004), was recently revealed to be a distinct species based on comparative genomic analysis (Haley et al. 2010). Additional environmental strains of this species have been isolated since then (Boucher et al. 2011). Also, since 2006, several clinical strains have been recovered from a range of specimen types (blood, stool, ear, and leg wound) and characterized by the Centers for Disease Control and Prevention (CDC, Atlanta, Georgia, USA). This recently described species, now officially called *V. metoecus* (Kirchberger et al. 2014), is even more closely related to *V. cholerae* than any other known *Vibrio* species based on biochemical and

genotypic tests (Boucher et al. 2011; Kirchberger et al. 2014). Previously, the closest known

relative of *V. cholerae* was *V. mimicus*, which was first described as a biochemically atypical

strain of *V. cholerae* and named after the fact that it "mimicked *V. cholerae*" phenotypically

(Davis et al. 1981).

The discovery of a closely related but distinct species which co-occurs with *V. cholerae*

in the environment (Boucher et al. 2011) presents a unique opportunity to investigate the

dynamics of interspecies interactions at the genetic level. In their environmental reservoir,

bacteria can acquire genetic material from other organisms as a result of horizontal gene

transfer (HGT; De la Cruz and Davies 2000). HGT plays an important role in the evolution,

adaptation, maintenance, and transmission of virulence in bacteria. It can launch

nonpathogenic environmental strains into new pathogenic lifestyles if they obtain the right

virulence factors. The two major virulence factors that have led to the evolution from

nonpathogenic to toxigenic *V. cholerae* are the cholera toxin (CTX), which is responsible for the

cholera symptoms (Waldor and Mekalanos 1996), and the toxin-coregulated pilus (TCP), which

is necessary for the colonization of the small intestine in the human host (Taylor et al. 1987).

These elements are encoded in genomic islands, specifically called pathogenicity islands, and

have been acquired horizontally by phage infections (Karaolis et al. 1999; Waldor and

Mekalanos 1996). Another genomic island, the integron, is used to capture and disseminate

gene cassettes, such as antibiotic resistance genes (Stokes and Hall 1989). Integrons have been

identified in a diverse range of bacterial taxa, and are known to play a major role in genome

evolution (Boucher et al. 2007; Mazel 2006). As evidenced by multiple HGT events across a wide

range of phylogenetic distances, integrons themselves, not only the cassettes they carry, may

have been mobilized within and between species throughout their evolutionary history

(Boucher et al. 2007). Integrons are ubiquitous among vibrios, but in some species, such as *V. cholerae*, it can occupy up to 3% of the genome and can contain over a hundred gene cassettes with a wide range of biochemical functions (Heidelberg et al. 2000; Mazel et al. 1998).

Here, we investigate the extent of genetic interaction between *V. metoecus* and *V. cholerae* through comparative genomic analysis, with the focus on the genomic islands, known hotspots for HGT (Dobrindt et al. 2004). The co-isolation of both species in the same environment (Boucher et al. 2011) indicates that *V. metoecus* is likely in constant interaction with *V. cholerae*. Our results show that there is a high rate of gene exchange between species, so rapid in the chromosomal integron that this region is indistinguishable between species. Multiple HGT events were also inferred in the core genome, including genes implicated in pathogenicity, with the majority with *V. metoecus* as a recipient of *V. cholerae* genes, suggesting a directional bias in interspecies gene transfer.

MATERIALS AND METHODS

Bacterial Strains Used

The *V. metoecus* and *V. cholerae* isolates sequenced in this study as well as genome sequences of additional isolates for comparison are listed in supplementary table S1. Environmental strains of *V. metoecus* and *V. cholerae* were isolated from Oyster Pond (Falmouth, Massachusetts, USA) on August and September 2009 using previously described methods

Downloaded from http://gbe.oxfordjournals.org/ at UPMC on January 29, 2016

SMBE

(Boucher et al. 2011). Isolates were grown overnight at 37°C in tryptic soy broth (Becton Dickinson, Sparks, Maryland, USA) with 1% NaCl (BDH, Toronto, Ontario, Canada). The sequences of the clinical *V. metoecus* strains were determined by the CDC (Atlanta, Georgia, USA). Additional sequences were obtained from the National Center for Biotechnology Information (Bethesda, Maryland, USA) GenBank database.

Genomic DNA Extraction and Quantitation

Genomic DNA was extracted from overnight bacterial cultures with the DNeasy Blood and Tissue Kit (QIAGEN, Hilden, Germany). The concentration for each extract was determined using the Quant-iT PicoGreen double-stranded DNA Assay Kit (Molecular Probes, Eugene, Oregon, USA) and the Synergy H1 microplate reader (BioTek, Winooski, Vermont, USA).

Genome Sequencing and Assembly

The genomic DNA extracts were sent to the McGill University and Génome Québec Innovation Centre (Montréal, Québec, Canada) for sequencing, which was performed using the TrueSeq library preparation kit and the HiSeq PE100 sequencing technology (Illumina, San Diego, California, USA). The contiguous sequences were assembled *de novo* with the CLC Genomics Workbench (CLC bio, Aarhus, Denmark). Functional annotations of the draft genomes were done in RAST v2.0 (Rapid Annotation using Subsystem Technology; Aziz et al. 2008).

6

Whole Genome Alignment

A circular BLAST atlas was constructed to visually compare whole genomes. The annotated genome sequences of *V. metoecus* and *V. cholerae* were aligned by BLASTN (Altschul et al. 1990) against a reference, *V. cholerae* N16961 (Heidelberg et al. 2000), using the CGView Comparison Tool (Grant et al. 2012).

Determination of Orthologous Gene Families and Pan-Genome Analysis

Orthologous groups of open reading frames (ORFs) from all strains of *V. metoecus* and *V. cholerae* were determined by pairwise bidirectional BLASTP using the OrthoMCL pipeline v2.0 (Li et al. 2003) with 30% match cutoff, since proteins sharing at least 30% identity are predicted to fold similarly (Rost 1999). The gene families were assigned into functional categories based on the Clusters of Orthologous Groups of proteins (COG) database (Tatusov et al. 2000). The pan- and core genome profiles for each species were determined with PanGP v1.0.1 (Zhao et al. 2014) using the distance guide algorithm, repeated 100 times. Sample size and amplification coefficient were set to 1,000 and 100, respectively.

Determination of Genomic Islands

The major genomic islands of *V. cholerae* N16961 were identified using IslandViewer (Langille and Brinkman 2009) and confirmed with previously published data (Chun et al. 2009;

Heidelberg et al. 2000). To determine if a putative homologue is present, ORFs in these genomic islands were compared against the ORFs of *V. metoecus* and *V. cholerae* by calculating the BLAST score ratio (BSR) between reference and query ORF (Rasko et al. 2005) using a custom-developed Perl script (National Microbiology Laboratory, Winnipeg, Manitoba, Canada). Only BSR values of at least 0.3 (for 30% amino acid identity) were considered (Rost 1999).

Determination of the Integron Regions

The chromosomal integron regions of *V. metoecus* and *V. cholerae* were recovered by finding the locations of the integron integrase gene *intI4* and the *attI* and *attC* recombination sites, identified with the ISAAC software (Improved Structural Annotation of *attC*; Szamosi 2012). The *intI4* and gene cassette sequences were used to calculate the ANI (Goris et al. 2007; Konstantinidis and Tiedje 2005) between strains (intra- and interspecies) in JSpecies v1.2.1 (Richter and Rosselló-Móra 2009), using the bidirectional best BLAST hits between nucleotides. The ANI of the integron region was compared to the ANI of 1,560 single-copy core ORFs (≈ 1.42 mbp).

Phylogenetic Analyses

Using the PhyloPhlAn pipeline v0.99 (Segata et al. 2013), 3,978 amino acid positions based on 400 universally conserved bacterial and archaeal proteins were determined. The concatenated alignment was used to construct a core genome maximum likelihood (ML) phylogenetic tree,

with a BLOSUM45 similarity matrix using the JTT+CAT amino acid evolution model optimized for topology/length/rate using NNI topology search. Robustness of branching was estimated with SH-like support values from 1,000 replicates.

Nucleotide sequences within a gene family were aligned with Clustal W v2.1 (Larkin et al. 2007), and an ML tree was constructed using RAxML v8.1.17 (Stamatakis 2014) using the GTR nucleotide substitution model and gamma distribution pattern. Robustness of branching was estimated with 100 bootstrap replicates. Interspecies gene transfer events were determined and quantified by comparison of tree topologies using the Phangorn package v1.99-11 (Schliep 2011) in R v3.1.2 (R Development Core Team 2014). A tree was partitioned into clades and determined whether the clades were perfect or not. Following the definition by Schliep and colleagues (2011), we defined a perfect clade as a partition that is both complete and homogeneous for a given taxonomic category (e.g., a clade with all *V. metoecus*, and only *V. metoecus*). At least one gene transfer event was hypothesized if a tree did not show perfect clades for neither *V. metoecus* nor *V. cholerae* (i.e., in a rooted tree, *V. metoecus* and *V. cholerae* are both polyphyletics).

Resulting alignments of the 1,184 single-copy core gene families not exhibiting HGT were concatenated, and alignment columns with at least one gap were removed using Geneious (Kearse et al. 2012). A final alignment with a total length of 771,455 bp was obtained and used to construct a core genome ML phylogenetic tree with RAxML v8.1.17 (Stamatakis 2014), as described above.

Genome Sequence Accession Numbers

The whole genome sequences generated in this study were deposited in the DNA Data Bank of Japan (DDBJ), European Molecular Biology Laboratory (EMBL), and GenBank databases. The accession numbers are listed in supplementary table S1. The versions described here are the first versions (XXXX01000000).

RESULTS AND DISCUSSION

V. cholerae is widely studied, and the genomes of globally diverse clinical and environmental isolates are available (supplementary table S1). On the other hand, there are currently only two *V. metoecus* genomes available. Strain RC341 was isolated from Chesapeake Bay (Maryland, USA) in 1998. It was presumptively identified as a variant *V. cholerae* based on 16S ribosomal RNA gene similarity to *V. cholerae* (Choopun 2004), but was later reclassified into its current species (Haley et al. 2010; Kirchberger et al. 2014). Strain OP3H was isolated in 2006 from Oyster Pond (Falmouth, Massachusetts, USA), a brackish pond in Cape Cod, Massachusetts. OP3H is considered the type strain of *V. metoecus*, which was recently officially described as a species (Kirchberger et al. 2014). A screen was performed for atypical *V. cholerae* isolates from a historical collection of clinical isolates at the CDC and identified that several of them were, in fact, *V. metoecus* (Boucher et al. 2011). Additional environmental *V. metoecus* strains were isolated in 2009 from Oyster Pond. While examining the population structure and surveying the mobile gene pool of environmental *V. cholerae* in Oyster Pond, Boucher and colleagues (2011)

discovered that both *V. metoecus* and *V. cholerae* co-occur in this location. To gain a better

understanding of the *V. metoecus* species, we sequenced the genomes of four clinical *V.

metoecus* strains originating from patients in the USA and an additional four from Oyster Pond.

To be able to evaluate genetic interactions between strains of two different species from the

same environment, we sequenced an additional twenty genomes of *V. cholerae* isolates from

the same Oyster Pond samples (fig. 1).

V. metoecus: The Closest Relative of V. cholerae

To obtain a visual comparison of the genomes, provide an overall impression of genome

architecture and identify highly conserved and divergent regions, a circular BLAST atlas was

constructed (Grant et al. 2012). *V. metoecus* and representative *V. cholerae* genomes were

compared by BLASTN alignment of coding sequences (Altschul et al. 1990) against the reference

V. cholerae N16961, a pandemic strain from Bangladesh isolated in 1971 whose entire genome

was sequenced to completion and carefully annotated (Heidelberg et al. 2000). The BLAST atlas

shows a clear distinction between species, as sequence identity is higher within a species than

between different species for most genes (fig. 2).

On average, *V. metoecus* shares 84% of its ORFs with *V. cholerae*, whereas 89-91% ORFs

are shared between strains of the same species (supplementary table S2). In contrast, *V.

mimicus*, previously the closest known relative of *V. cholerae*, shares only 64-69% of ORFs with

V. cholerae (Hasan et al. 2010). It was determined previously that the recommended cutoff

point for prokaryotic species delineation by DNA-DNA hybridization (DDH) is 70%, which

11

corresponds to 85% of conserved protein-coding genes for a pair of strains (Goris et al. 2007). These results show clear distinction between the three closely related species based on conserved genes, and *V. metoecus* is a much closer relative to *V. cholerae* than *V. mimicus*.

Another fundamental measure of relatedness between bacterial strains is ANI. This measure was proposed as a modern replacement to the traditional DDH method to determine relatedness of organisms, but still provide equivalent information (i.e., DNA-DNA similarity; Goris et al. 2007; Konstantinidis and Tiedje 2005). The ANI of the core genome is 86-87% between species and 98-100% within species (fig. 3*a*), showing a clear distinction between *V. metoecus* and *V. cholerae*. Two organisms belonging to the same species will have an ANI of at least 95%, corresponding to 70% DDH (Goris *et al.*, 2007), although earlier studies have proposed a 94% cutoff (Konstantinidis and Tiedje, 2005). For this reason, we have currently classified the clinical strain 07-2435 as *V. metoecus* as it shows 94% ANI with other *V. metoecus* strains but only 87% ANI with *V. cholerae* (fig. 3*a*).

A Portion of the Genome Escapes the Species Boundary Between *V. metoecus* and *V. cholerae*

The BLAST atlas allows for the clear distinction between strains belonging to the *V. cholerae* species and those belonging to the *V. metoecus* species. However, there is a clear and visible exception in one genomic region: the integron. Sequence identity of genes found in the integron region does not seem to differ within and between species (fig. 2).

The integron is a region of the genome capable of gene capture and excision (Stokes and Hall 1989) and can occupy up to 3% of the genome in *V. cholerae* (Heidelberg et al. 2000).

Although the size of the chromosomal integron region varies between isolates, there is no significant difference in length and number of ORFs between species and between clinical and environmental isolates (supplementary table S3). The ANI of the integron region was determined between pairs of strains and compared to the ANI of the core genome (fig. 3). While ANI is 86-87% between species and 98-100% within species for the core genome (fig. 3*a*), the integron region displays an average pairwise ANI of 93-94%, both within and between species (fig. 3*b*). Gene cassettes from the 10 *V. metoecus* and 11 *V. cholerae* integron regions were grouped into orthologous gene families, and the occurrence of HGT was quantified for gene families with at least two *V. metoecus* and *V. cholerae* members by the construction of phylogenetic trees. Of the 116 gene families considered, 109 or 94% do not show distinct separation between the two species in a phylogenetic tree. The high number of genes shared between species and their high nucleotide identity are likely the result of frequent interspecies HGT (fig. 2 and fig. 3*b*). A previous study by Boucher and colleagues (2011) showed that there is indeed a high frequency of gene exchange in the integron region between *V. cholerae* and *V. metoecus*, specifically from the same geographic location (i.e., *V. cholerae* and *V. metoecus* in Oyster Pond) as compared to the same species in different locations (i.e., *V. cholerae* from Bangladesh and the USA). Here, we show that not only is the frequency of interspecies HGT high in the integron, but that its level is such that this region becomes indistinguishable between species.

Although the functions of the majority of integron gene cassettes are unknown (Boucher et al. 2007), many of the known genes are antibiotic resistance genes and are implicated in the evolution of bacteria highly resistant to antibiotics (Collis and Hall 1995;

Rowe-Magnus and Mazel 2002). Looking into the predicted functions of the 116 gene families comprising 1,452 gene cassettes, the majority of which are shared between *V. metoecus* and *V. cholerae*, reveals genes that encode proteins involved in transport and metabolism of various molecules (supplementary fig. S1), suggesting a major contributing function of the integron for host acquisition and distribution of important resources in the environment by bacteria (Koenig et al. 2008). Gene cassettes encoding nicotinamidase-related amidases are present in multiple copies. Nicotinamidase catalyzes the deamination of nicotinamide to produce ammonia and nicotinic acid (Petrack et al. 1965). A key enzyme in many organisms, it has been shown to be important in the proliferation of bacteria pathogenic to mammalian hosts including humans (Kim et al. 2004; Purser et al. 2003). Other genes present are involved in basic cellular functions such as acetyltransferases, involved in post-translational modifications of ribosomal proteins, the functional significance of which remains unclear but may have regulatory roles (Nesterchuk et al. 2011). Some genes are part of the plasmid stabilization systems, which include the toxin-antitoxin (TA) systems. TA systems are frequently found in gene cassette arrays for the stabilization and prevention of loss of gene cassettes. They also play additional roles in stress response, bacterial persistence, and phage defense (Iqbal et al. 2015).

A Lack of Reciprocity: Directional Gene Flow from *V. cholerae* to *V. metoecus*

To get a quantitative estimate of the amount of HGT between *V. cholerae* and *V. metoecus,* we investigated the amount of interspecies recombination taking place in their core genomes. An ML tree was constructed for each of the 1,947 gene families comprising the *V. metoecus-V.*

cholerae core genome (fig. 4). The trees were then analyzed for gene transfer events by partitioning them into clades (Schliep 2011). In our analysis, following the definition by Schliep and colleagues (2011), a gene transfer is hypothesized if a member of one species clusters with members of the other species in a clade, and the tree cannot be partitioned into perfect clades, which must consist of all members from the same species and only of that species. Considering only the single-copy core genes, we have inferred interspecies HGT in 376 out of 1,560 genes (24%; supplementary table S4). Our analysis excluded 387 core genes that have duplicates in at least one of the genomes, as it is difficult to reliably assess HGT in genes from large paralogous families (Ge et al. 2005). Using this method, it was possible to determine directionality of HGT, whether from *V. cholerae* to *V. metoecus* or vice versa. HGT was qualified by examining the individual gene trees, and only reliable clustering with at least 70% bootstrap support was considered (Hillis and Bull 1993). A total of 655 interspecies gene transfer events were detected, with the majority (489 or 75%; p = 0.0053) with *V. metoecus* as the recipient (i.e., *V. metoecus* members clustering within the *V. cholerae* clade). On the other hand, we detected 166 (25%) of gene transfer events with *V. cholerae* as the recipient (supplementary table S5).

To investigate if this bias in directionality of HGT was due to differences in the origin or ecology of strains from one species or the other, we performed the analysis using only environmental strains from Oyster Pond. To ensure equal genetic diversity for both species, we compared the same number of isolates from each species. The 20 *V. cholerae* isolates we sequenced for this study can be grouped into five clonal complexes as determined by multilocus sequence typing of seven housekeeping genes. All the isolates from the same clonal complex cluster together in a core genome phylogenetic tree (fig. 1). They also exhibit 100%

15

ANI only with each other but not with isolates from other clonal complexes (supplementary table S6). Indeed, members of the same clonal complex always cluster together in all the individual gene trees examined (fig. 4). We therefore randomly chose one isolate from each *V. cholerae* clonal complex from Oyster Pond, yielding a final dataset of five genomes from each species. A total of 224 interspecies gene transfer events were detected in this environment-specific dataset, where 192 (86%; p = 0.0012) involved *V. metoecus* as the recipient and only 32 (14%) with *V. cholerae* as the recipient (table 1). One possibility to explain this bias could be that *V. cholerae* genes are more abundant in the environment and therefore more accessible to *V. metoecus*. Indeed, using culture-based methods, *V. cholerae* was 10 times more abundant than *V. metoecus* in Oyster Pond. Another possibility is that *V. cholerae* is more refractory to HGT as they contain more barriers to gene uptake, such as restriction-modification systems, or that *V. metoecus* is more permissive, containing more DNA uptake systems (conjugative plasmids, natural competence machinery or phages). However, no significant difference could be found in the number or nature of proteins involved in restriction-modification or DNA uptake systems between *V. metoecus* and *V. cholerae* in our study, although poorly transformable *V. cholerae*, despite having an intact and perfectly functioning DNA uptake system, have been reported (Katz et al. 2013). Additionally, nuclease activity by Dns, Xds, and other DNases can inhibit natural transformation (Blokesch and Schoolnik 2008; Gaasbeek et al. 2009). We also surveyed our *V. metoecus* and *V. cholerae* genomes for predicted DNases and found no significant difference between species.

Despite the directional gene transfer from *V. cholerae* to *V. metoecus*, it seems that the latter might have contributed to the virulence of its more famous relative by HGT. Interspecies

recombination was detected in four core genes where at least one clinical *V. cholerae* grouped in the same clade with *V. metoecus* (fig. 4). Interestingly, three of these genes are implicated, whether directly or indirectly, in *V. cholerae* pathogenesis. VC2614 encodes a cyclic-AMP regulatory protein, a global regulator of gene expression in *V. cholerae* including CTX and TCP (Skorupski and Taylor 1997). It appears that HGT in this case occurred in the ancestor of the phylocore genome (PG) group, which contains all pandemic strains (fig. 1; Chun et al. 2009), with a clinical *V. metoecus* strain as the possible donor. The new version of this cyclic-AMP regulatory protein was eventually lost in the classical O1 strain (O395). VC2545 encodes an inorganic pyrophosphatase, and its expression in *V. cholerae* may play an important role during human and mouse infection (Lombardo et al. 2007). This transfer was only between clinical *V. metoecus* and classical O1. VCA0925 encodes a dihydroorotase essential for pyrimidine biosynthesis. Biosynthesis of nucleotides is the single most critical metabolic function for growth of pathogenic bacteria in the bloodstream because of scarcity of nucleotide precursors but not other nutrients, and the genes involved serve as potential antibiotic targets for treatments of blood infection (Samant et al. 2008). Here, gene transfer involved not just the PG group of *V. cholerae*, but also the environmental strains of clonal complex 5 and 623-39.

Although these interspecies recombination events do not represent novel gene acquisitions, gaining a new allele of a gene can often have important consequences in a pathogen, changing its fitness in the host. This has been demonstrated for a single point mutation in *ompU*, *vpvC*, and *ctxB*. The *ompU* gene encodes for the major outer membrane porin OmpU, generally for the transport of hydrophilic solutes, but has been shown to provide *V. cholerae* resistance to bile acids and antimicrobial peptides in the host (Mathur and Waldor

2004; Provenzano et al. 2000). It is suggested that it can also act as a receptor for phage to infect *V. cholerae* (Seed et al. 2014). The *vpvC* gene encodes for diguanylate cyclase, and the mutation results in a switch from the smooth to rugose phenotype in *V. cholerae* (Beyhan and Yildiz 2007). The single point mutation in these genes results in a *V. cholerae* that is less susceptible to phage infection, contributing to the evolutionary success of the pathogen (Beyhan and Yildiz 2007; Seed et al. 2014). *V. cholerae* responsible for cholera outbreaks in Bangladesh have changing genotypes of *ctxB*, a subunit of CTX (Waldor and Mekalanos 1996), also caused by a single point mutation (Rashed et al. 2012). The years 2006 and 2007 saw a dominance of *V. cholerae* with the *ctxB* genotype 1 (*ctxB*1). *V. cholerae* with the *ctxB* genotype 7 (*ctxB*7) outcompeted *ctxB*1 from 2008-2012. However, there appears to be a shift back to *ctxB*1 since 2013. The changing *ctxB* genotypes were associated with differing levels of severity of cholera. This also suggests CTX phage-mediated evolution, survival, and dominance of *V. cholerae* (Rashid et al. 2015).

Components of Major Pathogenicity Islands are More Ancient than the *V. cholerae* Species

A BSR map (Rasko et al. 2005) was constructed to show the presence or absence of the genes comprising the major pathogenicity islands in various *V. metoecus* and *V. cholerae* isolates (fig. 5). Using the genes from *V. cholerae* N16961 as reference, BLASTP was used to determine the presence of homologous genes in the other strains (Altschul et al. 1990). The major *V. cholerae* virulence factors, CTX and TCP, which are encoded by pathogenicity islands that have been acquired horizontally by phage infections of the CTXΦ and VPIΦ, respectively (Karaolis et al.

1999; Waldor and Mekalanos 1996), are absent from all clinical and environmental *V. metoecus* (fig. 5*a*). The absence of CTX and TCP in *V. metoecus* is consistent with the absence of reports on a toxigenic *V. metoecus*.

Interestingly, our results show some of the other major pathogenicity islands to be present in some *V. metoecus* and non-pandemic *V. cholerae* strains in fragments and not as a complete presence or absence. This is evident in the *Vibrio* pathogenicity island 2 (VPI-2), which can be divided into four sub-clusters we call "islets," as indicated in fig. 5*a*. These four islets match the previous description of Jermyn and Boyd (2002) for VPI-2: (A) a type-1 restriction-modification system for protection against viral infection, (B) a *nan-nag* cluster for sialic acid metabolism, (C) a Mu phage-like region, and (D) a number of ORFs of unknown function. We hypothesize two scenarios as to the fragmentation of these genomic islands: (1) that the islands were obtained as a whole and sections were eventually lost, or (2) that the islands were acquired independently in islets and were accreted into the same region in the genome. Evolution would favor the latter hypothesis, as it is more parsimonious for fewer environmental strains to independently acquire certain islets of the islands rather than a majority of the strains acquiring whole islands and losing most regions eventually (Freeman and Herron 2007). Phylogenetic trees were constructed for the gene families that constitute the four putative islets of VPI-2. Gene trees for islet B, the *nan-nag* cluster, show distinct clustering of *V. metoecus* and *V. cholerae*, suggesting the acquisition of this region by a common ancestor, which diverged and evolved independently after speciation, with more recent isolated HGT events between *V. metoecus* and *V. cholerae* (fig. 5*b* and supplementary fig. S2). A similar pattern of distinct clustering of *V. metoecus* and *V. cholerae* is also observed in islet A, but the

latter is only present in O1 El Tor *V. cholerae* and two *V. metoecus* strains (fig. 5*a*), suggesting

that it was horizontally transferred between the two species and likely absent from their

common ancestor. Furthermore, islet C, the putative Mu phage-like region, is only detected in

V. cholerae of the PG group and TM 11079-80, an O1 El Tor environmental isolate. This islet is

absent in *V. metoecus*, which suggests a more recent acquisition of this region only by certain *V.*

cholerae. Lastly, islet D is prevalent in the majority of the isolates, whether *V. metoecus* or *V.*

cholerae, which do not cluster by species in the phylogeny (fig. 5*b*). This suggests frequent

interspecies HGT of its component genes. Taken together, these results support that the VPI-2

island emerged by accretion of smaller islets with different evolutionary histories before

reaching the form currently found in *V. cholerae* O1 El Tor or classical pandemic strains. The

nan-nag cluster (islet B) is likely ancestral, being present before speciation of *V. cholerae* and *V.*

metoecus, with islets A and D acquired later by the ancestor of pandemic *V. cholerae* through

HGT within or between species and islet C added most recently through HGT from an unknown

source.

The *Vibrio* seventh pandemic islands 1 and 2 (VSP-1 and VSP-2, respectively) are

genomic islands believed to be present and unique only among the seventh pandemic isolates

of *V. cholerae* (Dziejman et al. 2002; O'Shea et al. 2004). These VSPs are hypothesized to

provide a fitness advantage to these isolates. However, multiple variants of VSP-2 have been

detected in *V. cholerae*, including non-O1/O139 strains, by acquisition and loss of genes at

specific loci within a conserved core genomic backbone (Taviani et al. 2010). This core VSP-2 is

also present in two *V. metoecus* isolates, the clinical 2010V-1005 and environmental RC341 (fig.

5*a*), and may have been acquired from *V. cholerae*, as indicated by the great similarity of genes

in this region to *V. cholerae* and phylogenetic analysis (fig. 5*b* and supplementary fig. S3). This variant of VSP-2 is stable and present in diverse strains isolated from different times and geographic locations and may be the one circulating among non-O1/O139 isolates (Taviani et al. 2010). VSP-1 is present almost in its entirety in environmental *V. cholerae* VL426 and *V. metoecus* RC341 (fig. 5*a*); similar strains in the environment may serve as reservoirs of VSP-1. There is no correlation between the presence of VSP-1 and VSP-2 in non-O1/O139 *V. cholerae*, indicating that both islands were acquired independently in different HGT events by seventh pandemic *V. cholerae* (Taviani et al. 2010). The presence of both of the entire VSP-1 and the core of VSP-2 in *V. metoecus* strains indicate interspecies movement of pathogenicity islands, suggesting that interspecies transfer can contribute to the evolution of pathogenic variants.

Fundamental Genetic Differences Between *V. metoecus* and *V. cholerae*

To determine genetic differences between *V. cholerae* and *V. metoecus* and the unique gene content of each species, we first compiled their pan- and core genomes (supplementary fig. S4). The pan-genome is the entire gene repertoire of a bacterial species, whereas the core genome comprises genes shared by all the strains (Tettelin et al. 2005, Vernikos et al. 2015). ORFs from both species were assigned to orthologous groups based on sequence similarity, yielding pan- and core genomes containing 5,613 and 2,089 gene families, respectively, based on the 42 *V. cholerae* genomes used in this study (supplementary fig. S4*a*). This differs from the previous estimate of Chun and colleagues (2009), who determined the *V. cholerae* core genome to contain 2,432 gene families based on 23 strains, a higher core genome size than we obtained

from our dataset. The reduced core genome size is expected since the number of shared genes decreases with the addition of each new genome (Tettelin et al. 2005). It also depends on the degree of relatedness of the organisms. A study on 32 *Vibrionaceae* genomes, including 18 representative *V. cholerae*, established a core genome of only 1,000 gene families (Vesth et al. 2010). The *V. metoecus* pan- and core genomes constitute 4,298 and 2,872 gene families, respectively, based on the 10 genomes currently available (supplementary fig. S4*b*). The difference in pan- and core genome sizes of *V. cholerae* and *V. metoecus* can be explained by the significant difference in the number of genomes used. We expect the pan- and core genomes of *V. metoecus* to ultimately reach sizes similar to that of *V. cholerae* when genomes of additional strains become available.

As a newly described species, very little is currently known about the biology of *V. metoecus* and what sets it apart genetically from *V. cholerae*. From the combined pan-genome of both species, orthologous gene families present in various groups of strains were determined: families unique to *V. metoecus* and *V. cholerae*, or unique to clinical and environmental strains (supplementary fig. S5). Function was predicted for each gene family based on the COG database (supplementary fig. S6). *V. metoecus* contains more unique gene families than *V. cholerae* that are involved in carbohydrate transport and metabolism (supplementary fig. S6*a*). In the species description study by Kirchberger and colleagues (2014), it was determined that although the majority of biochemical and growth characteristics of *V. metoecus* resemble *V. cholerae*, the former was mainly differentiated from the latter for its ability to utilize the complex sugars D-glucuronic acid and *N*-acetyl-D-galactosamine. Indeed, multiple β-galactosidase/β-glucuronidase enzymes for the breakdown of D-glucuronic acid

(Louis and Doré 2014) were present in our *V. metoecus*-specific COG dataset, but not in *V. cholerae*. Multiple hexosaminidases for the hydrolysis of terminal *N*-acetyl-D-hexosamine (Magnelli et al. 2012) were also detected in *V. metoecus*, which supports the phenotype observed by Kirchberger and colleagues (2014). Additionally, genes unique for clinical *V. metoecus* and clinical *V. cholerae* were identified (supplementary fig. S6*b*). Clinical *V. cholerae* have more genes encoding proteins involved in replication, recombination, and repair (mostly transposases), and signal transduction, such as the GGDEF family protein. Transposases in pathogenicity islands can contribute to the instability and mobilization of virulence genes (Schmidt and Hensel 2004). The GGDEF family protein is critical in biofilm formation (García et al. 2004) and is highly induced in *V. cholerae* during infection in humans and mice (Lombardo et al. 2007). As expected, genes of the CTX and TCP clusters were not found in our clinical *V. cholerae*-specific dataset because they are not unique to clinical strains, but are also present in some environmental ones (fig. 5*a*). Among the genes uniquely found in clinical *V. metoecus* is a putative *mdaB* (modulator of drug activity B) gene. The *mdaB* gene has been shown to play an important role in oxidative stress resistance and host colonization in *Helicobacter pylori* (Wang and Maier 2004), and may also contribute to the fitness of clinical *V. metoecus* in the host.

CONCLUSION

The discovery of *V. metoecus*, the closest known relative of *V. cholerae*, presents an opportunity to study the HGT events between species and the role this might play in the evolution of pathogenesis. In contrast to the core genome, which is distinctly more similar

between members of the same species, the chromosomal integron region, occupying approximately 3% of *V. cholerae* and *V. metoecus* genomes, represents a pool of genes which is freely exchanged between these two species. This genomic region displays no greater similarity within than between species. Genomic islands encoding pathogenicity factors, known to play a role in pandemic *V. cholerae* virulence, are also occasionally found in *V. metoecus*, either completely or in part. This includes VPI-2, found in most pandemic *V. cholerae*, as well as the VSP islands, previously believed to be specific to *V. cholerae* strains from the seventh pandemic. VPI-2 and VSP-2 seem to have assembled over time by accretion of smaller units, which we call islets. Some islets, such as the *nan-nag* cluster of the VPI-2 (islet B) for sialic acid metabolism, have been stable over time and were present in the common ancestor of *V. metoecus* and *V. cholerae*. Other islets, such as islet A (restriction-modification system) and islet D (unknown function) of VPI-2, the core of VSP-2, or the entire VSP-1 island seem to move frequently between *V. metoecus* and *V. cholerae* and are not restricted to pandemic strains.

The most striking finding is that even the core genome of *V. cholerae* is susceptible to frequent interspecies recombination with *V. metoecus*. Twenty-four percent of the genes found in all *V. cholerae* and *V. metoecus* had experienced interspecies recombination. There also seems to be a directional bias to these recombination events. In Oyster Pond, in particular, *V. metoecus* is the recipient of genes six times more than *V. cholerae*. The cause of this bias is unclear, but it does not seem to be restricted to a single environment, as all *V. metoecus* are recipients of more interspecies DNA transfers than any of the *V. cholerae* strains investigated. One possibility is that *V. cholerae* is more abundant in most environments than *V. metoecus* and there is, therefore, simply more of its DNA available for uptake. Indeed, in this study, *V.*

cholerae was isolated 10 times more frequently than *V. metoecus* from Oyster Pond, which is consistent with the observed HGT bias. However, this explanation is very tentative and requires more evidence, since this study is the first one to isolate *V. cholerae* and *V. metoecus* quantitatively from the same site, and this was done using a culture-based method. This relative abundance would not necessarily be obtained with more accurate culture-free quantitative methods. Also, HGT could be biased because of differences in phage abundance/susceptibility, presence of DNA uptake systems, or restriction-modification systems. Nonetheless, this is, to our knowledge, the first quantitative report of HGT bias for bacteria in the natural environment and has fundamental implications for understanding the evolution of microbial populations.

ACKNOWLEDGMENTS

LITERATURE CITED

Ali M, et al. 2012. The global burden of cholera. Bull World Health Organ. 90:209-218A.

Altschul SF, Gish W, Miller W, Myers EW, Lipman DJ. 1990. Basic local alignment search tool. J Mol Biol. 215:403-410.

Aziz RK, et al. 2008. The RAST server: rapid annotations using subsystems technology. BMC Genomics. 9:75.

Beyhan S, Yildiz FH. 2007. Smooth to rugose phase variation in *Vibrio cholerae* can be mediated by a single nucleotide change that targets c-di-GMP signalling pathway. Mol Microbiol. 63:995-1007.

Blokesch M, Schoolnik GK. 2008. The extracellular nuclease Dns and its role in natural transformation of *Vibrio cholerae*. J Bacteriol. 190:7232-7240.

Boucher Y, et al. 2011. Local mobile gene pools rapidly cross species boundaries to create endemicity within global *Vibrio cholerae* populations. MBio. 2:e00335-10.

Boucher Y, Labbate M, Koenig JE, Stokes HW. 2007. Integrons: mobilizable platforms that promote genetic diversity in bacteria. Trends Microbiol. 15:301-309.

Choopun N. 2004. The population structure of *Vibrio cholerae* in Chesapeake Bay. Ph.D. Thesis. College Park: University of Maryland.

Chun J, et al. 2009. Comparative genomics reveals mechanism for short-term and long-term clonal transitions in pandemic *Vibrio cholerae*. Proc Natl Acad Sci USA. 106:15442-15447.

Collis CM, Hall RM. 1995. Expression of antibiotic resistance genes in the integrated cassettes of integrons. Antimicrob Agents Chemother. 39:155-162.

Davis BR, et al. 1981. Characterization of biochemically atypical *Vibrio cholerae* strains and designation of a new pathogenic species, *Vibrio mimicus*. J Clin Microbiol. 14:631-639.

De la Cruz F, Davies J. 2000. Horizontal gene transfer and the origin of species: lessons from bacteria. Trends Microbiol. 8:128-133.

Dobrindt U, Hochhut B, Hentschel U, Hacker J. 2004. Genomic islands in pathogenic and environmental microorganisms. Nat Rev Microbiol. 2:414-424.

Dziejman M, et al. 2002. Comparative genomic analysis of *Vibrio cholerae*: genes that correlate with cholera endemic and pandemic disease. Proc Natl Acad Sci USA. 99:1556-1561.

Freeman S, Herron JC. 2007. *Evolutionary Analysis*. San Francisco: Pearson Benjamin Cummings.

Gaasbeek EJ, et al. 2009. A DNase encoded by integrated element CJIE1 inhibits natural transformation of *Campylobacter jejuni*. J Bacteriol. 191:2296-2306.

García B, et al. 2004. Role of the GGDEF protein family in *Salmonella* cellulose biosynthesis and biofilm formation. Mol Microbiol. 54:264-277.

Ge F, Wang LS, Kim J. 2005. The cobweb of life revealed by genome-scale estimates of horizontal gene transfer. PLoS Biol. 3:e316.

Gomez-Gil B, et al. 2014. The family *Vibrionaceae*. In: Rosenberg E, DeLong EF, Lory S, Stackebrandt E, Thompson F, editors. *The Prokaryotes – Gammaproteobacteria*. Berlin: Springer. p. 659-747.

Goris J, et al. 2007. DNA-DNA hybridization values and their relationship to whole-genome sequence similarities. Int J Syst Evol Microbiol. 57:81-91.

Grant JR, Arantes AS, Stothard P. 2012. Comparing thousands of circular genomes using the CGView Comparison Tool. BMC Genomics. 13:202.

Haley BJ, et al. 2010. Comparative genomic analysis reveals evidence of two novel *Vibrio* species closely related to *V. cholerae*. BMC Microbiol. 10:154.

Hasan NA, et al. 2010. Comparative genomics of clinical and environmental *Vibrio mimicus*. Proc Natl Acad Sci USA. 107:21134-21139.

Heidelberg JF, et al. 2000. DNA sequence of both chromosomes of the cholera pathogen *Vibrio cholerae*. Nature. 406:477-483.

Hillis DM, Bull JJ. 1993. An empirical test of bootstrapping as a method for assessing confidence in phylogenetic analysis. Syst Biol. 42:182-192.

Iqbal N, Guérout AM, Krin E, Le Roux F, Mazel D. 2015. Comprehensive functional analysis of the 18 *Vibrio cholerae* N16961 toxin-antitoxin systems substantiates their role in stabilizing the superintegron. J Bacteriol. 197:2150-2159.

Jermyn WS, Boyd EF. 2002. Characterization of a novel *Vibrio* pathogenicity island (VPI-2) encoding neuraminidase (*nanH*) among toxigenic *Vibrio cholerae* isolates. Microbiology. 148:3681-3693.

Karaolis DK, Somara S, Maneval DR, Jr., Johnson JA, Kaper JB. 1999. A bacteriophage encoding a pathogenicity island, a type-IV pilus and a phage receptor in cholera bacteria. Nature. 399:375-379.

Katz LS, et al. 2013. Evolutionary dynamics of *Vibrio cholerae* O1 following a single-source introduction to Haiti. MBio. 4:e00398-13.

Kearse M, et al. 2012. Geneious Basic: an integrated and extendable desktop software platform for the organization and analysis of sequence data. Bioinformatics. 28:1647-1649.

Kim S, et al. 2004. *Brucella abortus* nicotinamidase (PncA) contributes to its intracellular replication and infectivity in mice. FEMS Microbiol Lett. 234:289-295.

Kirchberger PC, et al. 2014. *Vibrio metoecus* sp. nov., a close relative of *Vibrio cholerae* isolated from coastal brackish ponds and clinical specimens. Int J Syst Evol Microbiol. 64:3208-3214.

Koenig JE, et al. 2008. Integron-associated gene cassettes in Halifax Harbour: assessment of a mobile gene pool in marine sediments. Environ Microbiol. 10:1024-1038.

Konstantinidis KT, Tiedje JM. 2005. Genomic insights that advance the species definition for prokaryotes. Proc Natl Acad Sci USA. 102:2567-2572.

Langille MG, Brinkman FS. 2009. IslandViewer: an integrated interface for computational identification and visualization of genomic islands. Bioinformatics. 25:664-665.

Larkin MA, et al. 2007. Clustal W and Clustal X version 2.0. Bioinformatics. 23:2947-2948.

Li L, Stoeckert CJ, Jr., Roos DS. 2003. OrthoMCL: identification of ortholog groups for eukaryotic genomes. Genome Res. 13:2178-2189.

Lombardo MJ, et al. 2007. An *in vivo* expression technology screen for *Vibrio cholerae* genes expressed in human volunteers. Proc Natl Acad Sci USA. 104:18229-18234.

Louis P, Doré J. 2014. Functional metagenomics of human intestinal microbiome β-glucuronidase activity. In: Nelson KE, editor. *Encyclopedia of Metagenomics*. New York: Springer. p. 1-8.

Magnelli P, Bielik A, Guthrie E. 2012. Identification and characterization of protein glycosylation using specific endo- and exoglycosidases. Methods Mol Biol. 801:189-211.

Mathur J, Waldor MK. 2004. The *Vibrio cholerae* ToxR-regulated porin OmpU confers resistance to antimicrobial peptides. Infect Immun. 72:3577-3583.

Mazel D. 2006. Integrons: agents of bacterial evolution. Nat Rev Microbiol. 4:608-620.

Mazel D, Dychinco B, Webb VA, Davies J. 1998. A distinctive class of integron in the *Vibrio cholerae* genome. Science. 280:605-608.

Nesterchuk MV, Sergiev PV, Dontsova OA. 2011. Posttranslational modifications of ribosomal proteins in *Escherichia coli*. Acta Naturae. 3:22-33.

O'Shea YA, et al. 2004. The *Vibrio* seventh pandemic island-II is a 26.9 kb genomic island present in *Vibrio cholerae* El Tor and O139 serogroup isolates that shows homology to a 43.4 kb genomic island in *V. vulnificus*. Microbiology. 150:4053-4063.

Petrack B, Greengard P, Craston A, Sheppy F. 1965. Nicotinamide deamidase from mammalian liver. J Biol Chem. 240:1725-1730.

Provenzano D, Schuhmacher DA, Barker JL, Klose KE. 2000. The virulence regulatory protein ToxR mediates enhanced bile resistance in *Vibrio cholerae* and other pathogenic *Vibrio* species. Infect Immun. 68:1491-1497.

Purser JE, et al. 2003. A plasmid-encoded nicotinamidase (PncA) is essential for infectivity of *Borrelia burgdorferi* in a mammalian host. Mol Microbiol. 48:753-764.

R Development Core Team. 2014. R: a language and environment for statistical computing. Version 3.1.2. Vienna: R Foundation for Statistical Computing.

Rashed SM, et al. 2012. Genetic characteristics of drug-resistant *Vibrio cholerae* O1 causing endemic cholera in Dhaka, 2006-2011. J Med Microbiol. 61:1736-1745.

Rashid MU, et al. 2015. *ctxB*1 outcompetes *ctxB*7 in *Vibrio cholerae* O1, Bangladesh. J Med Microbiol. In press.

Rasko DA, Myers GS, Ravel J. 2005. Visualization of comparative genomic analyses by BLAST score ratio. BMC Bioinformatics. 6:2.

Richter M, Rosselló-Móra R. 2009. Shifting the genomic gold standard for the prokaryotic species definition. Proc Natl Acad Sci USA. 106:19126-19131.

Rost B. 1999. Twilight zone of protein sequence alignments. Protein Eng. 12:85-94.

Rowe-Magnus DA, Mazel D. 2002. The role of integrons in antibiotic resistance gene capture. Int J Med Microbiol. 292:115-125.

Samant S, et al. 2008. Nucleotide biosynthesis is critical for growth of bacteria in human blood. PLoS Pathog. 4:e37.

Schliep K, Lopez P, Lapointe FJ, Bapteste É. 2011. Harvesting evolutionary signals in a forest of prokaryotic gene trees. Mol Biol Evol. 28:1393-1405.

Schliep KP. 2011. Phangorn: phylogenetic analysis in R. Bioinformatics. 27:592-593.

Schmidt H, Hensel M. 2004. Pathogenicity islands in bacterial pathogenesis. Clin Microbiol Rev. 17:14-56.

Seed KD, et al. 2014. Evolutionary consequences of intra-patient phage predation on microbial populations. Elife. 3:e03497.

Segata N, Börnigen D, Morgan XC, Huttenhower C. 2013. PhyloPhlAn is a new method for improved phylogenetic and taxonomic placement of microbes. Nat Commun. 4:2304.

Skorupski K, Taylor RK. 1997. Cyclic AMP and its receptor protein negatively regulate the coordinate expression of cholera toxin and toxin-coregulated pilus in *Vibrio cholerae*. Proc Natl Acad Sci USA. 94:265-270.

Stamatakis A. 2014. RAxML version 8: a tool for phylogenetic analysis and post-analysis of large phylogenies. Bioinformatics. 30:1312-1313.

Stokes HW, Hall RM. 1989. A novel family of potentially mobile DNA elements encoding site-specific gene-integration functions: integrons. Mol Microbiol. 3:1669-1683.

Szamosi JC. 2012. ISAAC: an improved structural annotation of *attC* and an initial application thereof. M.Sc. Thesis. Hamilton: McMaster University.

Tatusov RL, Galperin MY, Natale DA, Koonin EV. 2000. The COG database: a tool for genome-scale analysis of protein functions and evolution. Nucleic Acids Res. 28:33-36.

Taviani E, et al. 2010. Discovery of novel *Vibrio cholerae* VSP-II genomic islands using comparative genomic analysis. FEMS Microbiol Lett. 308:130-137.

Taylor RK, Miller VL, Furlong DB, Mekalanos JJ. 1987. Use of *phoA* gene fusions to identify a pilus colonization factor coordinately regulated with cholera toxin. Proc Natl Acad Sci USA. 84:2833-2837.

Tettelin H, et al. 2005. Genome analysis of multiple pathogenic isolates of *Streptococcus agalactiae*: implications for the microbial "pan-genome". Proc Natl Acad Sci USA. 102:13950-13955.

Vernikos G, Medini D, Riley DR, Tettelin H. 2015. Ten years of pan-genome analyses. Curr Opin Microbiol. 23:148-154.

Vesth T, et al. 2010. On the origins of a *Vibrio* species. Microb Ecol. 59:1-13.

Waldor MK, Mekalanos JJ. 1996. Lysogenic conversion by a filamentous phage encoding cholera toxin. Science. 272:1910-1914.

Wang G, Maier RJ. 2004. An NADPH quinone reductase of *Helicobacter pylori* plays an important role in oxidative stress resistance and host colonization. Infect Immun. 72:1391-1396.

Zhao Y, et al. 2014. PanGP: a tool for quickly analyzing bacterial pan-genome profile. Bioinformatics. 30:1297-1299.

FIGURE LEGENDS

Figure 1. The phylogenetic relationship of the *V. metoecus* and *V. cholerae* strains. The ML phylogenetic tree was constructed from the concatenated sequence alignment of single-copy core gene families (771,455 bp). All reliable bootstrap support are indicated with * and are at least 97% for this tree. The scale bar represents nucleotide substitutions per site. Shortened branch lengths, approximately 3.5× the scale bar (0.175), are indicated. Strains with their genomes sequenced in this study are indicated by dots. Multiple *V. cholerae* strains from Oyster Pond (Massachusetts, USA) belong to the same clonal complex.

Figure 2. The *V. metoecus* (Vm) and *V. cholerae* (Vc) BLAST atlas. The map compares sequenced genomes against the reference (ref.), *V. cholerae* N16961. The two outermost rings show the forward and reverse strand sequence features of the reference. The next 33 rings show regions of sequence similarity detected by BLASTN comparisons between genes of the reference and query genomes. White regions indicate the absence of genes. Outermost black bars indicate the location of the major genomic islands. VSP – *Vibrio* seventh pandemic island; VPI – *Vibrio* pathogenicity island; CTX/TLC – cholera toxin/toxin-linked cryptic; chr. – chromosome; mbp – megabase pairs; kbp – kilobase pairs.

Figure 3. ANI of the core genome vs. chromosomal integron region of *V. metoecus* and *V. cholerae*. (*a*) Intra- and interspecies pairwise comparison of the 1,560 single-copy core genes (≈ 1.42 mbp). (*b*) Intra- and interspecies pairwise comparison of the integron gene cassettes.

Figure 4. Representative HGT between *V. metoecus* (Vm) and *V. cholerae* (Vc). The trees are representative ML phylogenetic trees from 1,560 orthologous families of single-copy core genes showing various examples of transfer events. Bottom trees: transfers involving at least one clinical *V. cholerae* clustering with *V. metoecus*. Relevant bootstrap support (>70%) is indicated with *. The scale bars represent nucleotide substitutions per site.

Figure 5. Virulence factors present in *V. metoecus* and *V. cholerae*. (*a*) The phylogenetic relationship of the *V. metoecus* and *V. cholerae* strains is shown on the left of each BSR map. The ML phylogenetic tree was constructed using 3,978 amino acid positions based on 400 universally conserved bacterial and archaeal proteins. The scale bars represent amino acid substitutions per site. The columns on the BSR maps show genes (locus tags) from genomic islands VPI-1, CTX/TLC, VPI-2, VSP-1, and VSP-2 of the reference, *V. cholerae* N16961. The black bars at the bottom of the BSR maps indicate the TCP cluster of VPI-1, *ctxAB* of CTX/TLC, islets of VPI-2, and core regions of VSP-2. The gradient bar shows the BSRs and their corresponding colours, with white regions indicating the absence of genes. Only BSR values of at least 0.3 were included. VPI – *Vibrio* pathogenicity island; CTX/TLC – cholera toxin/toxin-linked cryptic; VSP – *Vibrio* seventh pandemic island; RMS – restriction-modification system. (*b*) Representative ML phylogenetic trees of orthologous gene families of the VPI-2 islets and the VSP-2 core. Relevant bootstrap support (>70%) is indicated with *. The scale bars represent nucleotide substitutions per site. RE – restriction endonuclease.
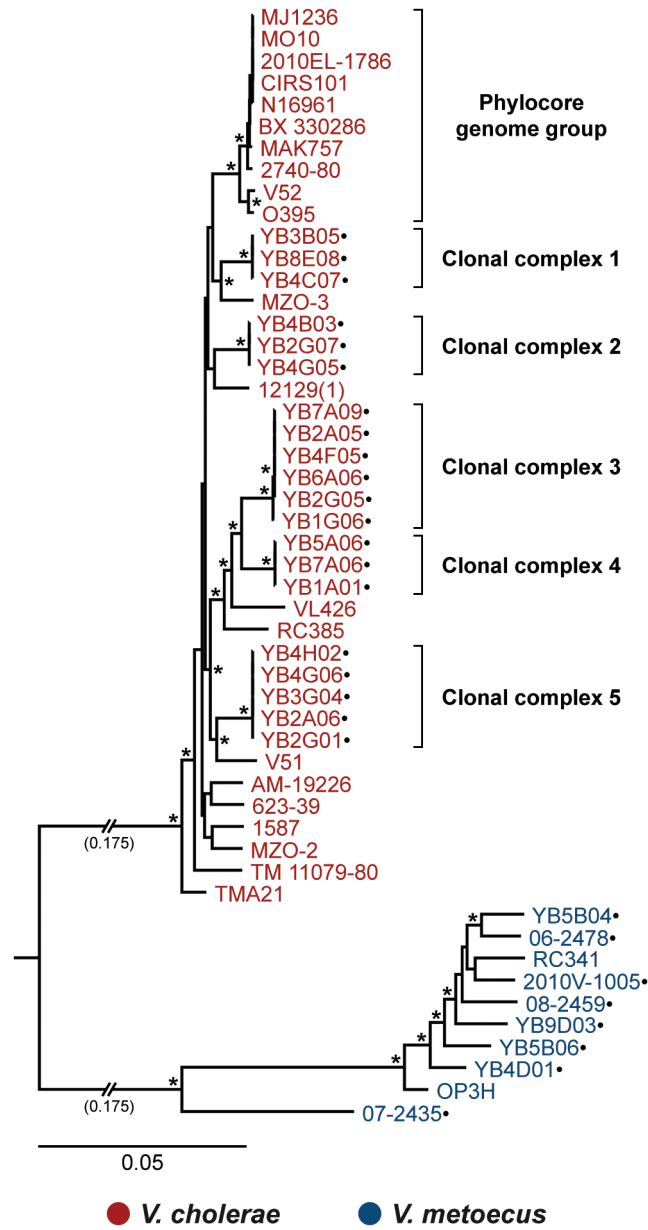
33

Figure 1

Phylocore
genome group

Clonal complex 1

Clonal complex 2

Clonal complex 3

Clonal complex 4

Clonal complex 5

0.05

● *V. cholerae* ● *V. metoecus*

Figure 2

Strains:
1) Vc N16961
2) Vc BX 330286
3) Vc MO10
4) Vc O395
5) Vc V52
6) Vc 2740-80
7) Vc 12129(1)
8) Vc YB3B05
9) Vc YB2G01
10) Vc AM-19226
11) Vc YB4B03
12) Vc TMA21
13) Vc TM 11079-80
14) Vc 623-39
15) Vc MZO-2
16) Vc 1587
17) Vc YB4F05
18) Vc YB7A06
19) Vc MZO-3
20) Vc VL426
21) Vc RC385
22) Vc 877-163
23) Vc V51
24) Vm 07-2435
25) Vm YB5B04
26) Vm 06-2478
27) Vm 2010V-1005
28) Vm YB5B06
29) Vm YB9D03
30) Vm 08-2458
31) Vm OP3H
32) Vm YB4D01
33) Vm RC341

Ref.: *V. cholerae* N16961
Chr. I - 2.96 mbp
Chr. II - 1.07 mbp

BLAST Hit:
- ■ = 100% identical
- ■ ≥ 98% identical
- ■ ≥ 96% identical
- ■ ≥ 94% identical
- ■ ≥ 92% identical
- ■ ≥ 90% identical
- ■ ≥ 88% identical
- ■ ≥ 86% identical
- ■ ≥ 84% identical
- ■ ≥ 82% identical
- □ > 0% identical

Figure 3

(a) Core Genome

V. cholerae   *V. metoecus*

(b) Integron

V. cholerae   *V. metoecus*

Legend: ANI = 100%   ANI ≥ 98%   ANI ≥ 96%   ANI ≥ 94%   ANI ≥ 92%   ANI ≥ 90%   ANI ≥ 88%   ANI ≥ 86%

Figure 4

● *V. cholerae*   ● *V. metoecus*

VC0432
Malate dehydrogenase
(no transfer)

VCA1002
AzlC family protein
(multiple Vm with Vc)

VC2407
Penicillin-binding protein
(one Vc/Vm with other species)

VCA0291
Integron integrase
(clinical Vm with Vc)

VC2614
Cyclic-AMP regulatory protein
(Vc PG group with Vm)

VC2545
Inorganic pyrophosphatase
(clinical Vc/Vm with
other species)

VCA0925
Dihydroorotase
(multiple Vc/Vm with
other species)

VC2459
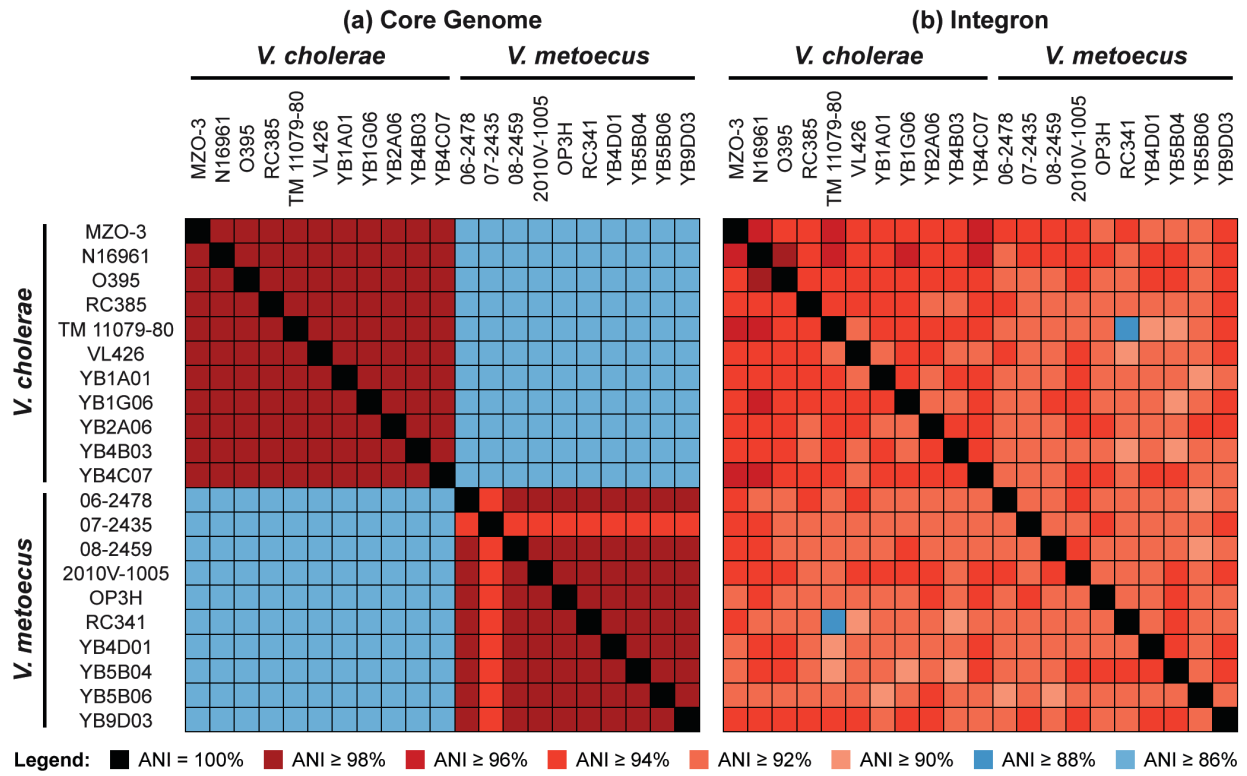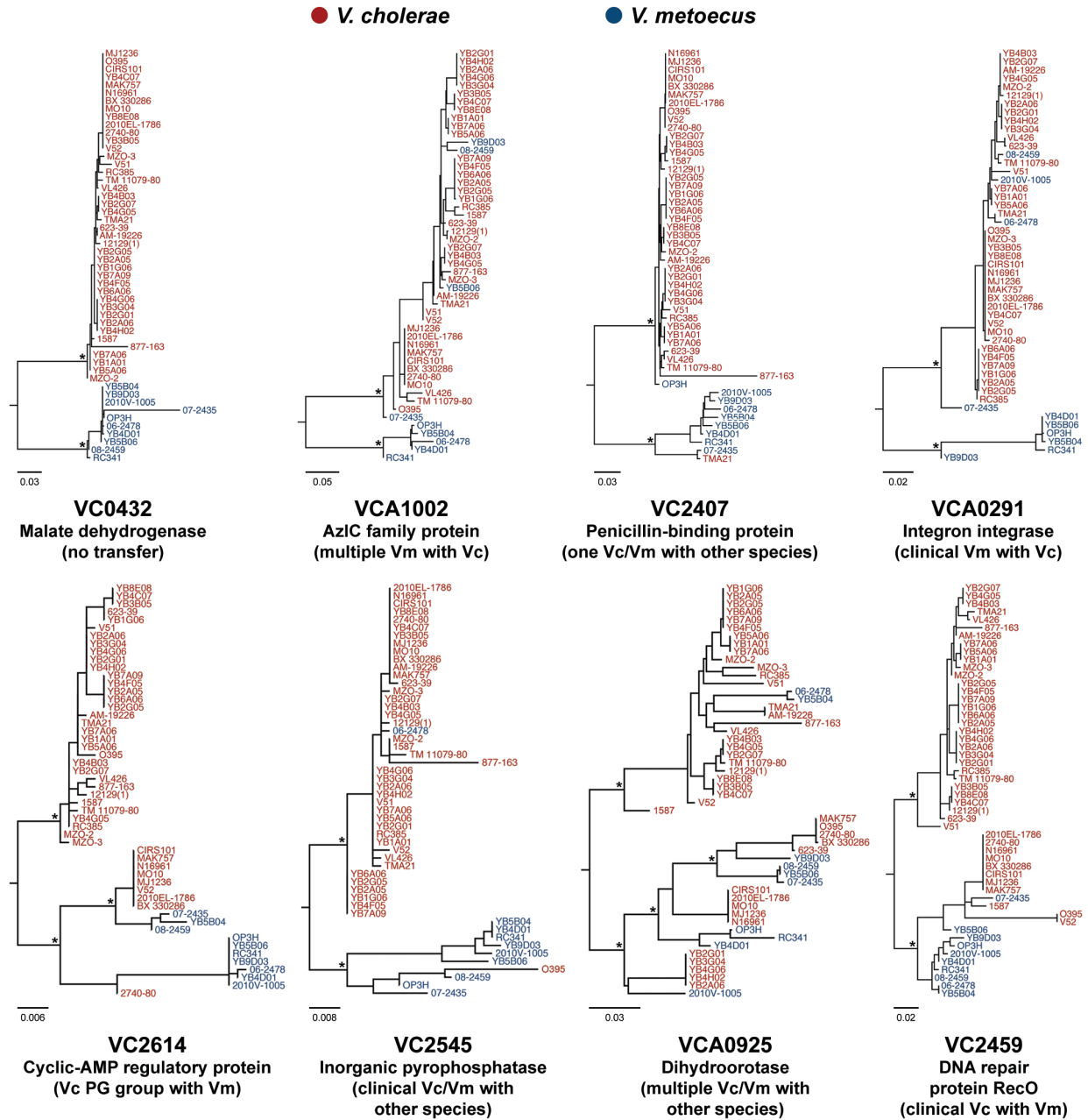DNA repair
protein RecO
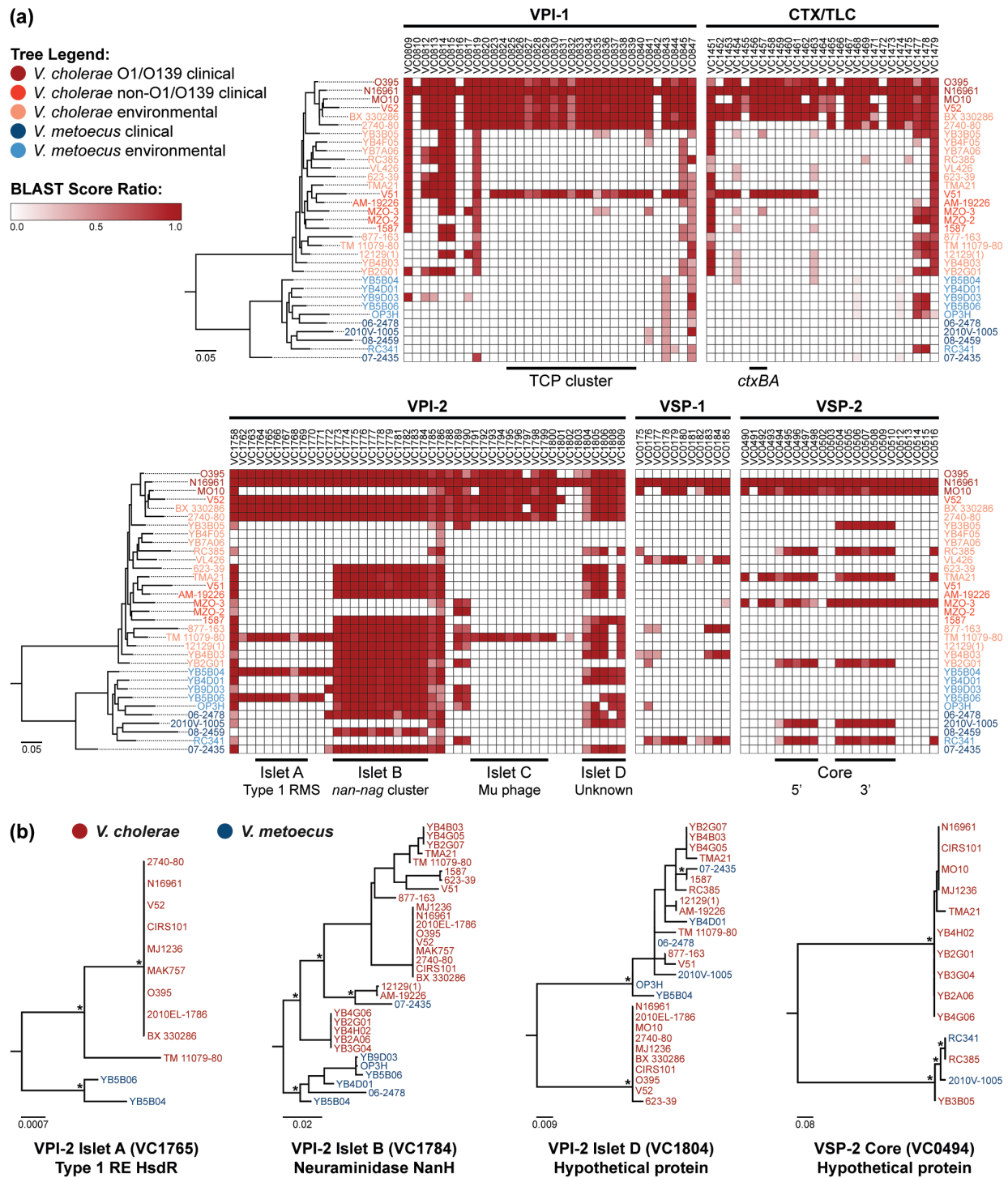(clinical Vc with Vm)

Figure 5

38

Table 1. HGT count for *V. metoecus* and representative *V. cholerae* strains from Oyster Pond (Massachusetts, USA) based on 376 single-copy core genes with inferred HGT. Only one strain from each clonal complex (CC) was included. An HGT event was hypothesized when a strain clustered with members of the other species in a phylogenetic tree, with reliable bootstrap support (>70%). Unequal variance *t*-test, *p* = 0.0012.

Species and Strain	HGT Count	Percent of Total
V. metoecus OP3H	55	25%
V. metoecus YB4D01	43	19%
V. metoecus YB5B06	37	17%
V. metoecus YB5B04	30	13%
V. metoecus YB9D03	27	12%
	192	**86%**
V. cholerae YB2G01 (CC 5)	16	7%
V. cholerae YB4F05 (CC 3)	9	4%
V. cholerae YB4B03 (CC 2)	4	2%
V. cholerae YB7A06 (CC 4)	2	1%
V. cholerae YB3B05 (CC 1)	1	0%
	32	**14%**